

# Topological Index Theorem on the Lattice through the Spectral Flow of Staggered Fermions

V. Azcoiti,<sup>\*</sup> E. Follana,<sup>†</sup> and A. Vaquero<sup>‡</sup>

*Universidad de Zaragoza.*

G. Di Carlo<sup>§</sup>

*INFN, Laboratori Nazionali del Gran Sasso.*

(Dated: July 27, 2021)

## Abstract

We investigate numerically the spectral flow introduced by Adams for the staggered Dirac operator on realistic (quenched) gauge configurations. We obtain clear numerical evidence that the definition works as expected: there is a clear separation between crossings near and far away from the origin, and the topological charge defined through the crossings near the origin agrees, for most configurations, with the one defined through the near-zero modes of large taste-singlet chirality of the staggered Dirac operator. The crossings are much closer to the origin if we improve the Dirac operator used in the definition, and they move towards the origin as we decrease the lattice spacing.

---

<sup>\*</sup> azcoiti@azcoiti.unizar.es

<sup>†</sup> efollana@unizar.es

<sup>‡</sup> Alejandro.Vaquero@mib.infn.it; present address: INFN, Sezione di Milano-Bicocca.

<sup>§</sup> giuseppe.dicarlo@lngs.infn.it

## I. INTRODUCTION

As is well known, smooth  $SU(N)$  gauge fields in a 4-dimensional compact differentiable manifold  $M$  have associated an integer topological charge

$$Q = -\frac{1}{32\pi^2} \int_M d^4x \epsilon_{\mu\nu\rho\sigma} \text{tr} [F_{\mu\nu} F_{\rho\sigma}] \quad (1)$$

where  $F_{\mu\nu}$  is the gauge potential.

This is not merely a mathematical curiosity; it plays a fundamental role in the understanding of the  $U_A(1)$  problem through the anomaly [1–3], and the Witten-Veneziano formula [4, 5]. It is also crucial for the investigation of the  $\theta$  vacuum in QCD and the strong CP problem [6], and therefore with the current experimental searches for axions [7, 8].

The issue of obtaining a theoretically sound and practical definition for the topological charge of lattice gauge fields is an old one. Several definitions exist, each with its own advantages and disadvantages. Some such definitions are purely gluonic, essentially transcribing the continuum definition to the lattice, whereas others take advantage of the index theorem and compute the charge as the index of a conveniently chosen fermionic operator.

In [9], Adams introduced a new definition of the index of a staggered Dirac operator, based on the spectral flow of a related hermitian operator. Some numerical results were obtained there for synthetic configurations in the  $2D$   $U(1)$  model.

The purpose of this paper is to study systematically Adams' definition in 4D (quenched) QCD (preliminary results were presented in [10]).

## II. DEFINITION OF THE TOPOLOGICAL CHARGE

The basic observation of Adams in [9] is that when considering the spectral flow definition of the topological charge in the continuum, there is some freedom in the choice of the relevant hermitian operator. By a suitable choice, we can construct an operator which, when implemented in the lattice with a staggered dirac operator has all the required properties.

In the continuum, for a given gauge field, one usually considers the spectral flow of the hermitian operator

$$H(m) = \gamma_5 (D - m) \quad (2)$$

as a function of  $m$ . Because of the key property that

$$H(m)^2 = D^\dagger D + m^2, \quad (3)$$

if we trace the flow of eigenvalues  $\{\lambda(m)\}$  of  $H$ , the ones corresponding to the zero modes of  $D$ , and only those, will change sign at the origin  $m = 0$ , each with a slope  $\pm 1$  which depends on the chirality of the corresponding mode. This gives us the index of  $D$ , and through the index theorem, the topological charge  $Q$  of the corresponding gauge configuration.

On the lattice, we can substitute in (2)  $D$  by the discretized Wilson Dirac operator

$$H_W(m) = \gamma_5 (D_W - m) \quad (4)$$

Now the index can be obtained similarly to the continuum, by counting the number of eigenvalues of  $H(m)$  that change sign close to the origin  $m = 0$ , taking into account the slope of such crossings. If we try to do the same with the lattice staggered Dirac operator  $D_{st}$ , we realize that the procedure does not work anymore, as the corresponding  $H$  fails to be hermitian.

The key innovation in Adams [9] is the realization that one can use a different  $H$  in the continuum to accomplish the same task, namely

$$H(m) = iD - m\gamma_5. \quad (5)$$

This operator is hermitian and verifies (3), and therefore its spectral flow also gives the index of  $D$ . But now we can substitute in (5)  $D$  by the lattice staggered discretization,

$$H_{st}(m) = iD_{st} - m\Gamma_5, \quad (6)$$

where  $D_{st}$  is the massless staggered Dirac operator and  $\Gamma_5$  is the taste-singlet staggered  $\gamma_5$  [11]. This operator is hermitian, and we can study its spectral flow,  $\lambda(m)$ . The would-be zero modes of  $D_{st}$  are identified with the eigenmodes for which the corresponding eigenvalue flow  $\lambda(m)$  crosses zero at low values of  $m$ , and the chirality of any such mode equals (with our conventions) the sign of the slope of the crossing [9].

Any staggered discretization of the Dirac operator can be used, in principle, to implement 6. We have chosen to work with the unimproved, 1-link staggered Dirac operator [12], and with the highly improved HISQ discretization [13]. In each case we have calculated, using standard numerical algorithms, the smallest (in absolute value) 20 eigenvalues of  $H_{st}(m)$

for enough values of  $m$  to allow us to determine unambiguously the cuts with the  $x$  axis. To compare with previous work, we have also calculated the low-lying modes of the HISQ Dirac operator at  $m = 0$ , and identify the would-be zero modes with the high taste-singlet chirality ones [14, 15].

### III. 2D U(1)

We started by studying the behavior of the spectral flow of  $H_{st}(m)$  corresponding to the 1-link staggered Dirac operator in 2D U(1) lattice gauge theory; our purpose was twofold: testing our numerical framework in a less demanding setting, and working in a theory with a simple geometrical definition of the topological charge (even if not immune from problems arising from dislocations [16]). To this end we can either construct gauge fields configurations with an assigned topological charge [17], or generate realistic field configurations from a canonical ensemble, selecting those with the charge  $Q$  we are interested in. We used the first possibility in the earlier stage of our tests and then we moved to the other option: the results shown in what follows are from this second phase<sup>1</sup>.

We have generated a large ensemble of quenched configurations at different values of  $\beta$ , varying from 4 to 9, in order to cover the scaling region for the lattice size we consider ( $L=60$ ). Then we select among this set of configurations subsets of fixed charge  $Q$ , for which we computed the spectral flow.

The spectrum of (6) has the exact symmetry  $\lambda(m) \leftrightarrow -\lambda(-m)$ , therefore we only need to calculate the flow for, say,  $m > 0$ . An equal number of crossings, with identical slopes, will be present for  $m < 0$ .

In Fig. 1 we show the spectral flow for a gauge configuration with a charge  $Q = -2$ , corresponding to a  $12^2$  lattice and a coupling constant  $\beta = 4.0$ . We plot the lowest (in absolute value) 20 eigenvalues of  $H(m)$  in the range  $(-3, 3)$ . We can appreciate two crossings with negative slopes for  $m < 0$ , and the symmetric ones for  $m > 0$ <sup>2</sup>.

In Fig. 2 we show the spectral flows corresponding to several gauge configurations in a larger volume,  $60^2$ , and at several values of the coupling. From now on we only plot the flow

---

<sup>1</sup> See [18] for related work in the unquenched case.

<sup>2</sup> Staggered fermions in  $D$  dimensions have a taste degeneracy of  $2^{D/2}$ , and therefore the number of crossings in the continuum gets multiplied by that factor in the lattice.

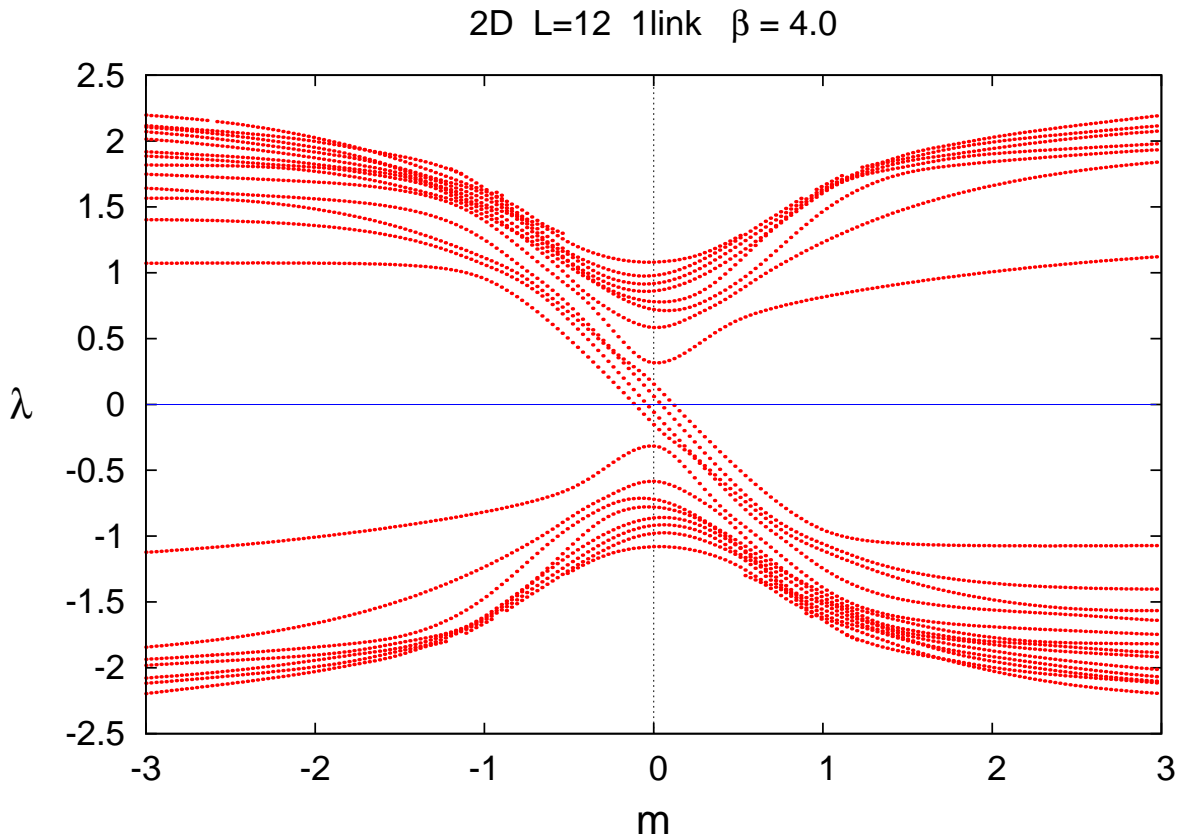


FIG. 1. Spectral flow of the 2D 1link Dirac operator for a gauge configuration with  $Q = -2$ .

for  $m > 0$ . For clarity, in most of the figures we plot the variable

$$\tilde{\lambda} = \text{sgn}(\lambda)\sqrt{|\lambda|}\log(|\lambda|) \quad (7)$$

versus  $\log(m)$ . As we can see in every case we have the expected number of crossings.

#### IV. 4D QUENCHED QCD

For our numerical calculations in 4D we have used three ensembles of tree-level Symanzik and tadpole improved quenched QCD at three values of the coupling constant  $\beta$  (5.0, 4.8 and 4.6), corresponding respectively to lattice spacings of approximately 0.077, 0.093 and 0.125 fm [15], with lattice volumes of  $20^4$ ,  $16^4$  and  $12^4$  respectively. These ensembles are thus approximately matched in physical volume,  $\approx 1.5\text{fm}^4$ .

In Figs. 3 and 4 we show the spectral flow for several representative configurations from the coarsest and finest ensembles, and in each case for  $H_{st}$  built from both the 1-link and

2D L=60 1link

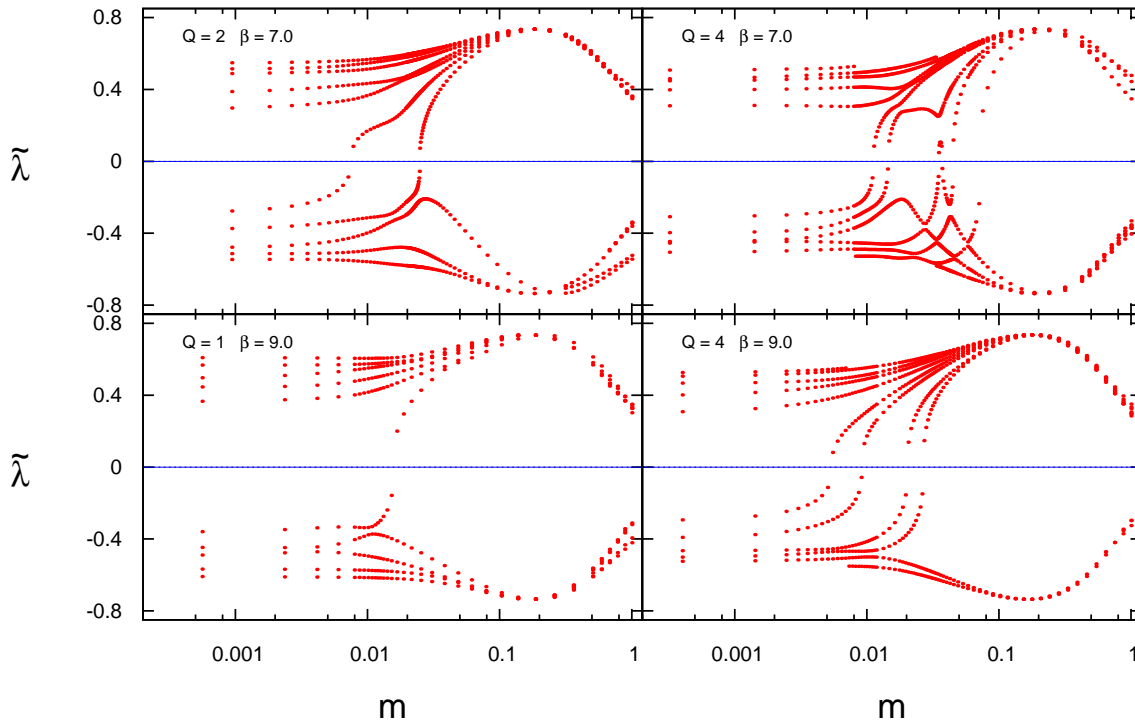


FIG. 2. Comparison of the spectral flow of the 2D 1link Dirac operator for several gauge configurations.

the HISQ Dirac operators. As before, we calculate the first 20 eigenvalues in absolute value. The topological charges were also calculated by counting the number of eigenvectors of the HISQ Dirac operator with high chirality [15], and in each case there is agreement between the two definitions and for the spectral flow corresponding to both operators. We can appreciate in the figures that the cuts of the spectral flow with the x axis are closer to the origin  $m = 0$  for the HISQ than for the 1-link operators, and also get closer as we go to smaller lattice spacings. This is consistent with the expectation that in the continuum limit the cuts should move to the origin, and that the improved Dirac operator is closer to the continuum than its unimproved counterpart. In order to make a more quantitative statement, we have computed a histogram (normalized to area one) of the cuts for the three different ensembles and both operators, which is shown in Fig. 5. We can see clearly the large differences between both operators, and how the distribution of cuts moves towards

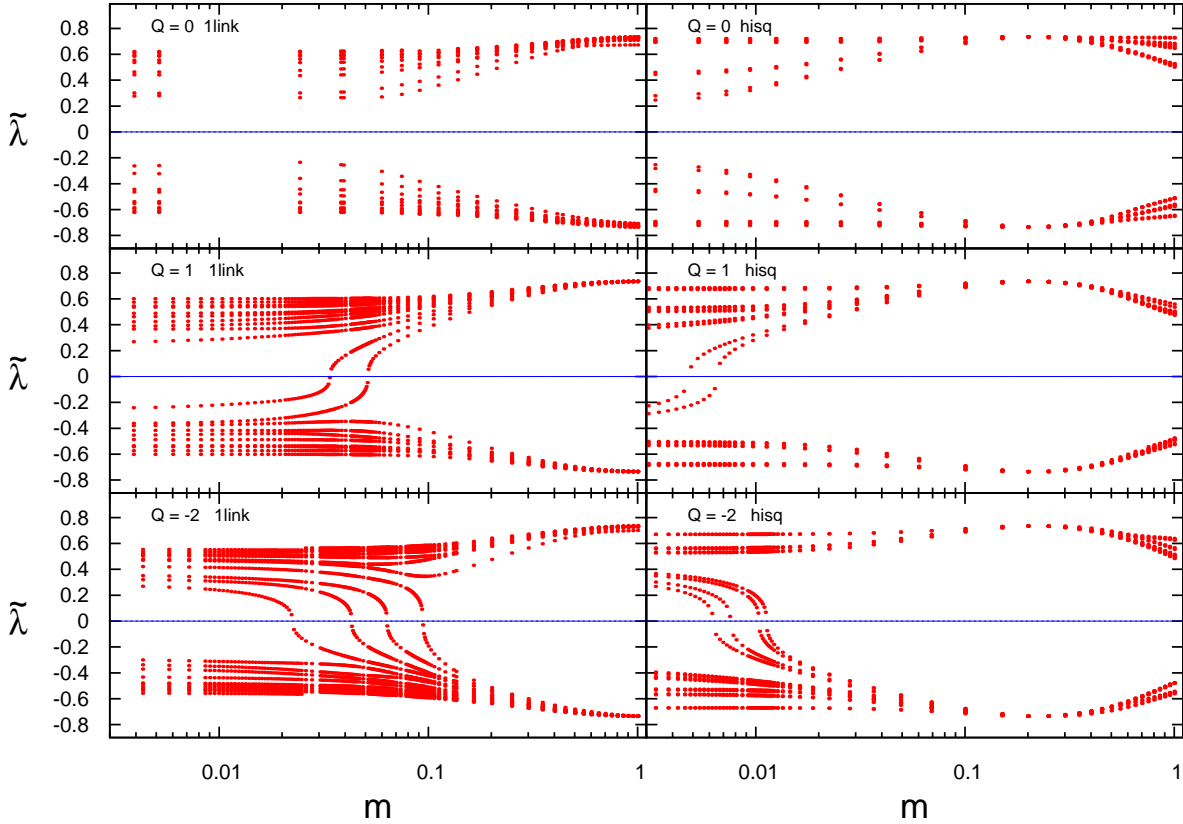


FIG. 3. Spectral flow for several configurations at  $\beta = 4.6$  (coarse ensemble) and for various values of the topological charge. The left and right panels correspond to the spectral flow calculated on the same configuration but with a different operator.

zero as we decrease the lattice spacing.

In order for the identification of the topological charge through the spectral flow to be unambiguous, it is necessary that there is a clear separation between cuts close and far away from the origin. To test whether this is the case we have calculated a few flows up to very large values of the parameter  $m$ . We show in Fig. 6 a representative result corresponding to a fine configuration, for both the unimproved and the HISQ cases. We can see that there is a very clear separation between cuts close to the origin and other possible cuts, which are very far away from the origin for both operators.

We have also calculated the spectral flow corresponding to the Wilson Dirac operator for a few configurations, in order to compare the results with the staggered case. We have chosen to do the comparison with the flow corresponding to the 1-link operator, which is

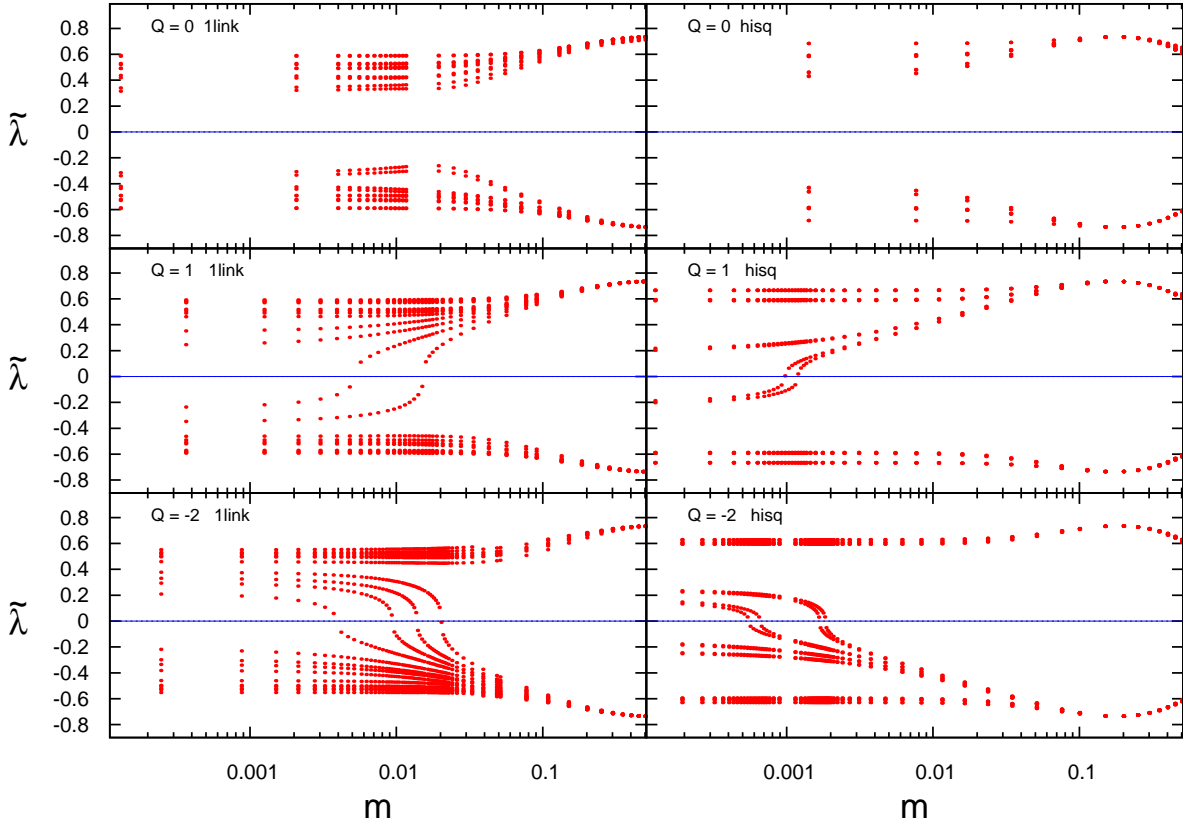


FIG. 4. Spectral flow for several configurations at  $\beta = 5.0$  (fine ensemble) and for various values of the topological charge. The left and right panels correspond to the spectral flow calculated on the same configuration but with a different operator.

unimproved, and therefore in a sense a closer relative to the Wilson one. In Figs. 7 and 8 we show both the Wilson and the 1-link staggered flow for two configurations corresponding to the coarsest and finest ensembles, both with  $Q = -1$ . As we can see we get consistent results in both cases. On the other hand, the computer time needed for the calculation is considerably less in the staggered case, possibly due to the better conditioning of the staggered Dirac operator.

## V. CONCLUSIONS AND OUTLOOK

We have presented clear numerical evidence that Adams' definition of the topological charge using the staggered Dirac operator works as expected also for realistic (quenched)  $SU(3)$  gauge fields. The crossings near and far away from the origin are very well separated,



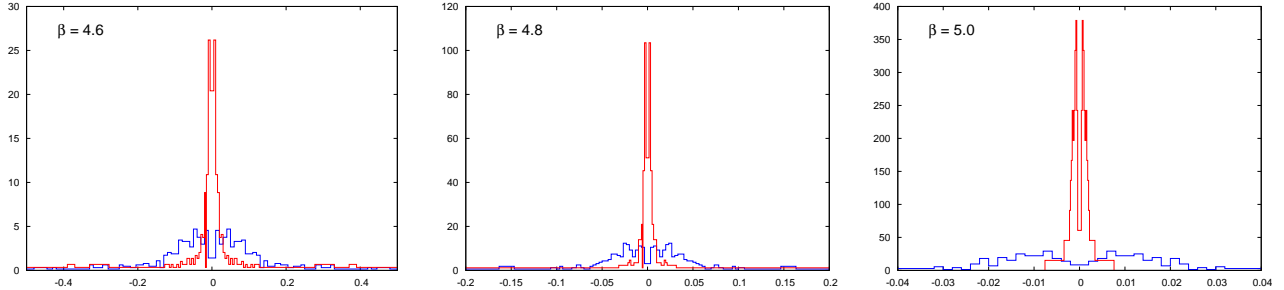


FIG. 5. Normalized histograms of the distribution of cuts of the spectral flow with the zero x axis for the three ensembles. In each individual figure we have plotted both the 1link result (broad distribution) and the HISQ result (narrow distribution) on the same scale for comparison. Scales are different for the different figures.

and therefore the topological charge of a configuration is unambiguously defined, even in cases which would be ambiguous using other definitions. For most configurations we have seen that the charge as measured by the number of high taste-singlet chirality modes and by the spectral flow agree. We have also seen the expected differences between the position of the cuts between the 1link and the HISQ operators, as well as the clear move towards zero of the cuts as we decrease the lattice spacing.

For a future work, it would be interesting to repeat this study in full QCD ensembles, including the effect of sea quarks.

Inspired by this construction, it is possible to define an overlap operator starting with a staggered kernel, instead of the usual Wilson one [19], producing a chiral operator representing two tastes of fermions. A similar construction can be carried out to further reduce the degeneracy and produce a one-flavor overlap operator [20]. The question is whether this construction has all the required properties, and is further numerically advantageous as compared with the usual overlap construction. Results are presented in [21–24].

## ACKNOWLEDGMENTS

We thank Alistair Hart for generating the configurations. This work was funded by an INFN-MICINN collaboration (under grant AIC-D-2011-0663), MICINN (under grants FPA2009-09638, FPA2008-10732 and FPA2012-35453, cofinanced by the EU through FEDER funds), DGIID-DGA (grant 2007-E24/2), and by the EU under ITN-STRONGnet

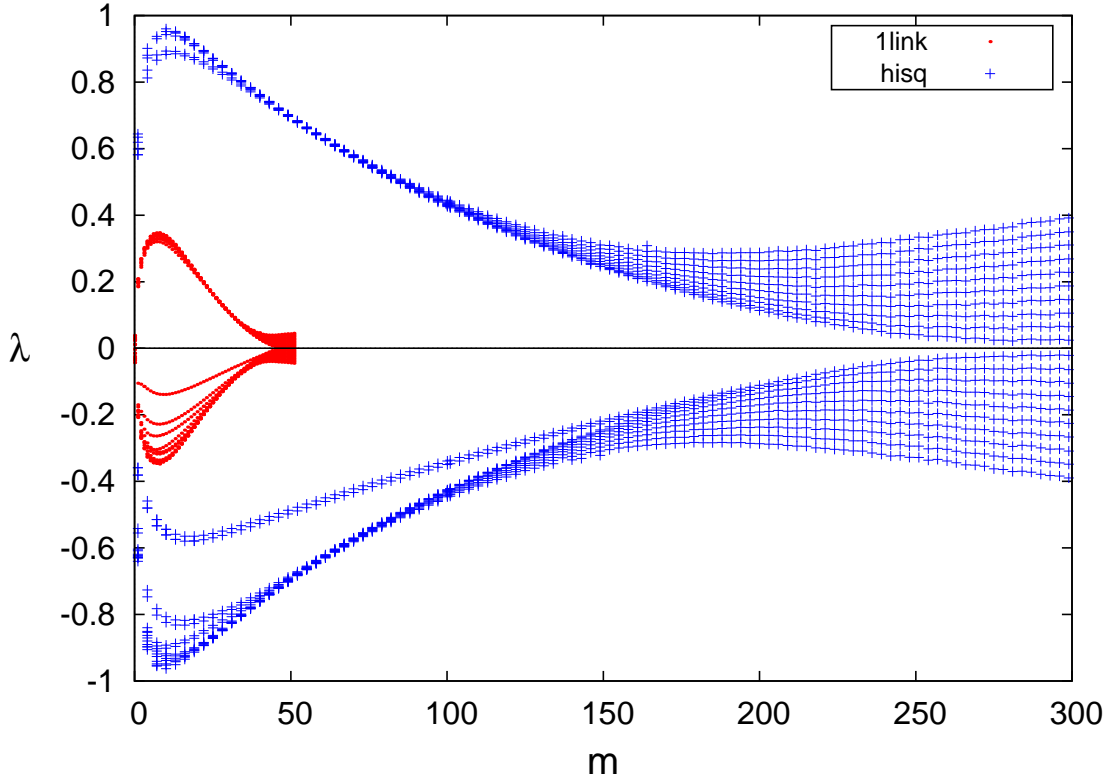


FIG. 6. Spectral flow for very large values of  $m$  for a typical configuration in the fine ensemble, both for the 1link and the HISQ staggered operators.

(PITN-GA-2009-238353). E. Follana was supported on the MICINN Ramón y Cajal program. and A. Vaquero was supported by MICINN through the FPU program. E. Follana acknowledges financial support from the Laboratori Nazionali del Gran Sasso during several research visits where part of this work was carried out.

- 
- [1] S. Adler, Phys. Rev. **117** (1969) 47.
  - [2] J.S. Bell, R. Jackiw, Nuov. Cim. **60A** (1969) 529.
  - [3] G. 't Hooft, Phys. Rev. Lett. **37** (1976), 8.
  - [4] E. Witten, Nucl. Phys. **B156** (1979) 269.
  - [5] G. Veneziano, Nucl. Phys. **B159** (1979) 213.
  - [6] R.D. Peccei, H.R. Quinn, Phys. Rev. Lett. **38** (1977) 1440.
  - [7] J. E. Kim, G. Carosi, Rev. Mod. Phys. **82** (2010) 557. [arXiv:0807.3125].

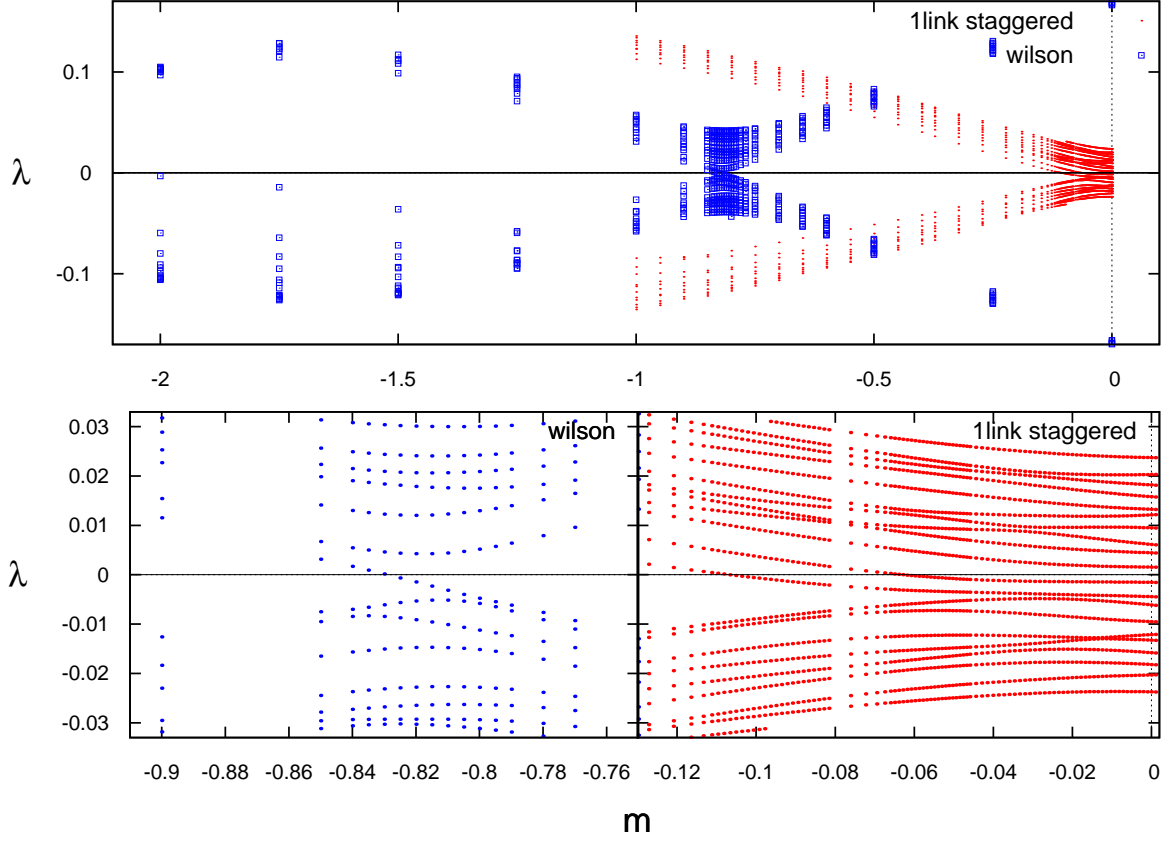


FIG. 7. Comparison of the Wilson and the staggered flow for the same configuration of charge  $Q = -1$  in the coarse ensemble. The lower figures are a detailed view of the crossings with the  $x$  axis.

- [8] O. Wantz, E. P. S. Shellard Phys. Rev. **D82**, (2010) 123508. [arXiv:0910.1066].
- [9] D. H. Adams, Phys. Rev. Lett. **104** (2010) 141602. [arXiv:0912.2850].
- [10] E. Follana, V. Azcoiti, G. Di Carlo, A. Vaquero, **PoS LATTICE2011** 100 (2011). [arXiv:1111.3502].
- [11] M. F. L. Golterman, Nucl. Phys. **B273** (1986) 663.
- [12] J. Kogut, L. Susskind, Phys. Rev. **D11** (1975) 395.
- [13] E. Follana Q. Mason, C.T.H. Davies, K. Hornbostel, G.P. Lepage, J. Shigemitsu, H. Trotter, K. Wong, Phys. Rev. **D75** (2007) 054502. [hep-lat/0610092].
- [14] E. Follana, A. Hart, C.T.H. Davies, Phys. Rev. Lett. **93** (2004) 241601. [hep-lat/0406010].
- [15] E. Follana, A. Hart, C.T.H. Davies, Q. Mason, Phys. Rev. **D72** (2005) 054501. [hep-lat/0507011].

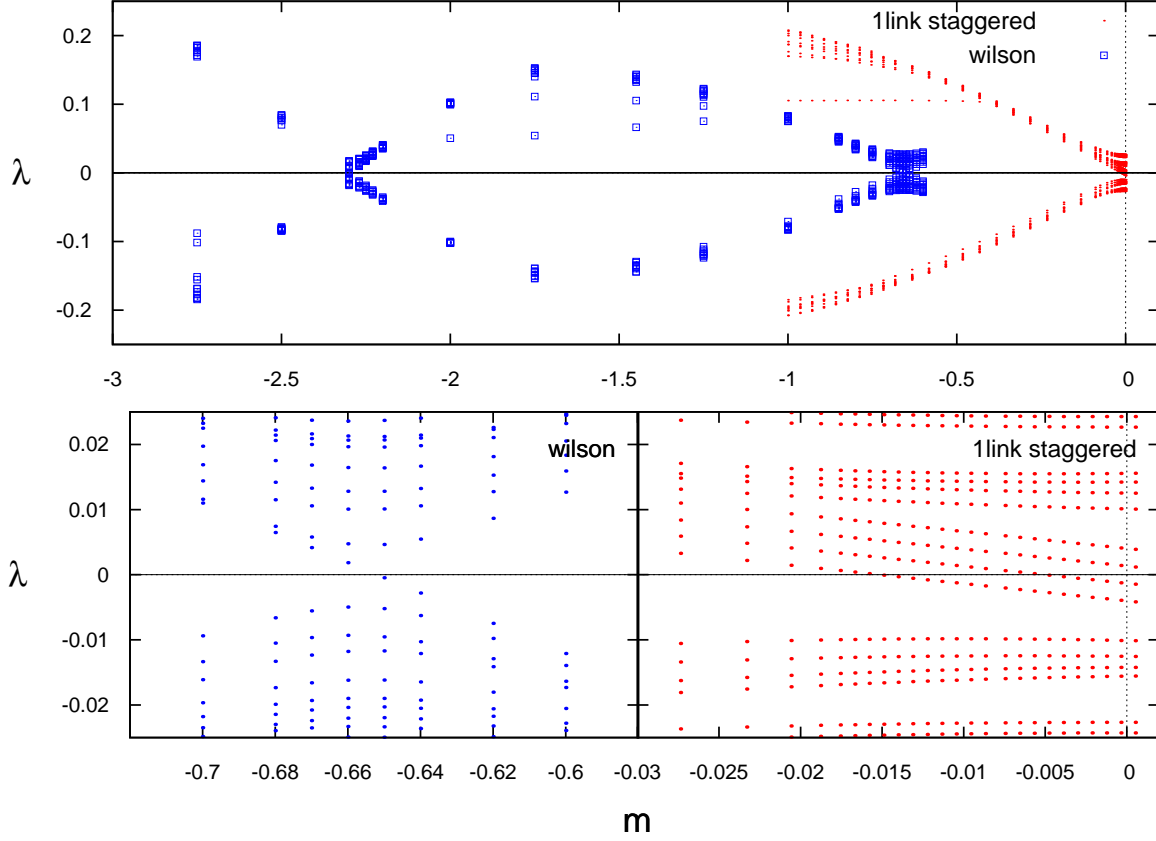


FIG. 8. Comparison of the Wilson and the staggered flow for the same configuration of charge  $Q = -1$  in the fine ensemble. The lower figures are a detailed view of the crossings with the x axis.

- [16] M. Teper, Phys. Lett. **162B** (1985) 357; 171B (1986) 81, 86.
- [17] J. Smit, J.C. Vink, Nucl. Phys. **B286** (1987) 485.
- [18] S. Dürr, Phys.Rev. **D85** (2012) 114503. [arXiv:1203.2560].
- [19] D. H. Adams, Phys. Lett. **B699** (2011) 394-397. [arXiv:1008.2833].
- [20] C. Hoelbling, Phys. Lett. **B696** (2011) 422-425. [arXiv:1009.5362].
- [21] P. de Forcrand, A. Kurkela, M. Panero, PoS **LATTICE2010** (2010) 080. [arXiv:1102.1000].
- [22] P. de Forcrand, A. Kurkela, M. Panero, JHEP **1204** (2012) 142. [arXiv:1202.1867].
- [23] S. Dürr, Phys. Rev. **D87** (2013) 114501. [arXiv:1302.0773].
- [24] D. H. Adams, R. Har, Y. Jia, C. Zielinski, PoS **LATTICE2013** (2013). [arXiv:1312.7230].